Molecular Weight Characterization of Poly(*N*-isopropylacrylamide) Prepared by Living Free-Radical Polymerization

François Ganachaud,[†] Michael J. Monteiro,[†] Robert G. Gilbert,*[,†] Marie-Anne Dourges,[‡] San H. Thang,[§] and Ezio Rizzardo[§]

Key Centre for Polymer Colloids, Chemistry School, Sydney University, NSW 2006, Australia; Laboratoire de Chimie Macromoléculaire, UMR 7610, Université Pierre et Marie Curie, 4 Place Jussieu, 75252 Paris Cedex 05, France; and CSIRO Molecular Science, Bag 10 Clayton South, Victoria 3169, Australia

Received February 18, 2000; Revised Manuscript Received June 16, 2000

ABSTRACT: A series of relatively monodisperse samples of poly(*N*-isopropylacrylamide) were synthesized by reversible addition−fragmentation chain transfer (RAFT) over the molecular weight range 2×10^3−3×10^5. For molecular weights below 4×10^4, conditions were found so that polydispersity remained below 1.4 up to high conversion (72%). Molecular weight distributions of polymer obtained using GPC in THF and MALDI were in accord for the low molecular weight range (typically 10^5). Particular care is required in GPC sample preparation: it is necessary to ensure that trace amounts of water are initially present when drying a polymer sample prior to dissolution in THF, to avoid irreversible chain aggregation. The log/log plot of intrinsic viscosity against molecular weight for polyNIPAM was found to be linear for molecular weights $<10^5$, after which the hydrodynamic volume seems to be independent of molecular weight. The Mark−Houwink parameters obtained from the lower molecular weight data are $K = 10^{-(4.24\pm0.42)}$ dL g^{-1} and $a = 0.78 \pm 0.09$.

Introduction

Water-soluble polymers have many applications. For example, polymers exhibiting different properties with variations of external parameters such as pH and temperature have created interest in biomolecule vectorization;[1] as one instance, using 3-mercaptopropionic acid[2−4] as a transfer agent can be used to prepare well-controlled functional end-chain polymers, which are then used to graft selective biomolecules on polymer colloids.

N-Isopropylacrylamide (NIPAM) is a water-soluble monomer whose polymer exhibits many fascinating properties.[5] It mimics the molecular structure of amino acids,[6] and its polymer exhibits a coil-to-globule transition at 32 °C (the LCST, lower critical solution temperature). This property is the result of the rather complex polarity of this molecule. Below the LCST, the amide functionality imbibes water molecules, via hydrogen bonding, giving it both its water solubility and surface activity. However, moving above the transition temperature breaks these hydrogen bonds, and the polymer expels water molecules and undergoes a coil-to-globule transition, thereby precipitating to form particles.

Controversies surround the GPC analysis of polyNIPAM. Some authors[7] claim that this method cannot be used to obtain molecular weight information for this polymer, due to filtration problems encountered before the analysis (suggesting the possibility of chain entanglements being so strong that significant numbers of chains may be caught up in the filter before entering the GPC column). Others only use GPC results to explain their average end functionality.[3] Schild[8] in his review specifically avoided the description of GPC analyses because of these inconsistencies.

The literature[3,4,9−17] shows that molecular weight distributions obtained by THF-phase GPC (based on polystyrene calibration) are in accord with other methods used in the low molecular weight range, such as end-chain titration.[3,4] On the other hand, for higher molecular weights, GPC generally gives lower apparent molecular weights than those obtained using light scattering,[18−21] viscosity[4,6,7,13,14,22−25] (using Mark−Houwink−Sakaruda parameters given in the literature), and osmometry.[2,19,26] A comparison between data obtained from GPC and from other methods performed on the same samples is shown in Figure 1. Discrepancies observed at low molecular weights might be attributed to nonideal variation of hydrodynamic volume with molecular weight. However, such a correction would be physically inapplicable for higher molecular weights (typically above 5×10^4).

To our knowledge, only one group has reported GPC traces in both water and THF.[9,11] Samples of different molecular weight ranges were obtained by performing the syntheses in different mixtures of benzene (or toluene) and THF, which is a very efficient transfer agent.[9,11] Some obvious differences are seen in the data from these authors. The shape of the peak is very different for the two solvents, that for polyNIPAM in THF being highly asymmetric. In addition, a large discrepancy was found in the polydispersity index, water-based GPC giving a much broader distribution than a THF-based one.

The primary objective of the present paper is to understand and resolve this anomaly in the measurement of molecular weight distributions. In principle, triple-detector SEC can be used for this purpose, but the many difficulties associated with this technique for "well-behaved" polymers[27,28] suggest that alternatives should be sought for a "difficult" polymer like polyNIPAM. The best means of resolution would appear to be the preparation of polyNIPAM samples with

[†] Chemistry School.
[‡] Université Pierre et Marie Curie.
[§] CSIRO Molecular Science.

10.1021/ma0003102 CCC: $19.00
Published on Web 08/09/2000

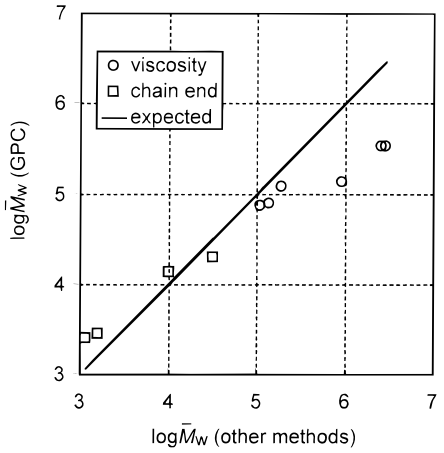

Figure 1. Points represent comparison of $\bar{M}_w$ values from the literature obtained by GPC (with methanol or THF as eluent with polystyrene standards) and from other methods: chain-end titrations[3,4,14] and viscosity.[2−4,14] Line represents values expected if all methods gave same result.

Scheme 1

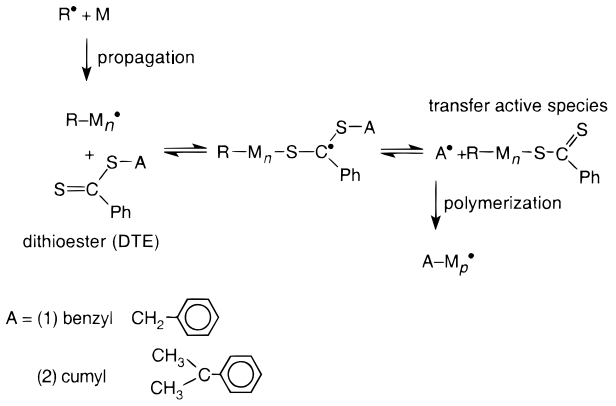

molecular weight distributions that are sufficiently monodisperse to be used to determine the Mark−Houwink−Sakaruda parameters accurately. Ionic "living" polymerization of NIPAM has been attempted, but protecting and deprotecting the active amide centers has been fraught with difficulty.[8,29] The best means of making monodisperse samples would appear to be to make use of one of the so-called "living" free-radical controlled polymerization techniques that are becoming available. To date, NIPAM has not been successfully polymerized using such methods, although other (meth)-acrylamides have been synthesized by ATRP with limited success.[30]

Reversible addition−fragmentation chain transfer (RAFT) is a living free-radical polymerization process for producing molecular weight distributions with narrow polydispersities (usually <1.2).[31−35] This process has the distinct advantage over other conventional free-radical living processes (e.g., nitroxide,[36] reversible atom and group transfer[37]) in that it can be used for a wide range of monomers, which can be polymerized in a wide range of solvents under a wide range of experimental conditions. The RAFT process involves the addition of monomer, a good solvent for both monomer and polymer, an azo or peroxy initiator, and the essential ingredient of a reversible transfer agent. A simplified mechanism is given in Scheme 1, together with the chemical structures of the two transfer agents used in this work. The transfer agent (dithioester, DTE) reacts with the initiator-derived radical (R•) or the propagating radical (R−M$_n$•) to give another transfer agent and the species A•, which reinitiates polymerization. The living behavior involves a reversible addition−fragmentation sequence between the active and dormant species with the S=C(Ph)S− moiety.

Table 1. RAFT Polymerization Conditions at 60 °C[a]

series	[NIPAM], M	[AIBN], mM	[DTE], mM	x, %	polymerization rate/10^{-6}, M s^{-1}
1a	0.892	0.293	4.324	10	0.62
1b			2.162	8	1.24
1c			1.081	35	3.61
1d			0.541	30	9.29
1e			0.270	8.8	7.27
2a	1.780	0.117	3.926	14	8.65
2b				38	11.74
2c				56	11.54
2d				72	7.42
3a	1.780	0.606	0.521	76	23.64
3b			1.041	56	17.46
3c			1.560	80	9.89
3d			2.080	68	8.41
3e			2.600	60	7.42
control	0.892	0.293	0	50	41.30

[a] Series **1** and **3** are polymerized in the presence of benzene and benzyl dithiobenzoate, and series **2** is polymerized in the presence of 1,4-dioxane and cumyl dithiobenzoate. x = conversion.

The purpose of the present work was to prepare polyNIPAM with narrow MWDs over a wide range of molecular weights and use these to obtain Mark−Houwink−Sakaruda parameters and elucidate the problems of GPC characterization of the polymer. These data will be used in a subsequent paper to obtain information on the propagation rate coefficient using pulsed-laser polymerization.

In brief, the procedure adopted here to find the MHS parameters is as follows. Samples from a series of RAFT polymerizations are analyzed using MALDI and intrinsic viscosity. If the RAFT polymerizations follow ideal kinetics, the molecular weight distribution should be narrow and linear with time, whence $\bar{M}_n$ can be obtained entirely from conversion data. The MALDI results, which are for moderately low molecular weight samples, show that the system indeed follows this expectation to an adequate approximation. The [η] data, which are for a wider range of molecular weights, show a linear Mark−Houwink plot (wherein the molecular weights are those predicted from ideal RAFT kinetics), whence the MHS parameters are obtained. GPC data are then used to provide consistency tests of these inferences.

Experimental Section

Materials. NIPAM (Wako) was recrystallized twice in a benzene/hexane mixture. The initiator (AIBN) was used after recrystallization in methanol. The two dithioesters used in this study, benzyl dithiobenzoate and cumyl dithiobenzoate (see Scheme 1), were synthesized using methods described elsewhere.[38,39] Two solvents were used in the RAFT polymerization: benzene (Aldrich, 99%) and 1,4-dioxane (Aldrich, 99%). THF (Unichrom, AR Grade, >99%) was used for GPC characterization.

RAFT Procedure. AIBN-initiated solution polymerization of NIPAM was carried out under two sets of conditions (see Table 1). The first set used benzyl dithiobenzoate and benzene (series 1 and 3), and the second used cumyl dithiobenzoate and 1,4-dioxane (series 2). Samples were freeze−thawed three times to remove oxygen, flame-sealed, and placed in a water bath at 60 °C. For the series of polymerizations carried out in 1,4-dioxane, the resulting polyNIPAM was purified by addition of the reaction mixture to a small amount of acetone, which was then added dropwise to petroleum ether, and gently

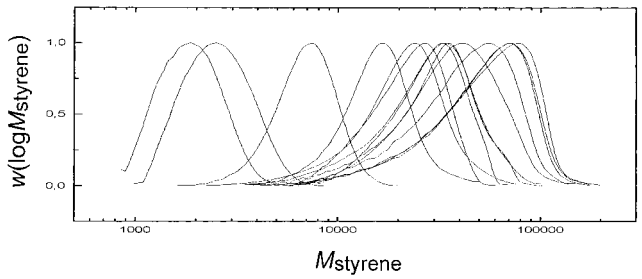

Figure 2. GPC distributions $w(\log M)$, based on polystyrene standards, for the samples given in Table 1. GPC chromatograms are obtained using two columns. The increase in molecular weight corresponds to a decrease in the dithioester concentration.

warmed above 40 °C until the polymer precipitated. This process was shown to be an adequate purification technique by checking with ^{1}H NMR.

Sample Preparation Prior to GPC Injection. PolyNIPAM (0.2−4.8 mg) was dissolved in 5 mL of water. This solution was then placed in an oven at 50−60 °C (i.e., above its LCST) and dried until the solution was no longer turbid (after ∼5 h); up to the LCST, polyNIPAM chains spontaneously precipitate to form microgel structures with a water content of ∼10−20%, and when the solution ceases to be turbid, this means that the "external" water has gone, and the only water that remains is the ≲20% that effectively prevents chain aggregation. THF was then added and allowed to evaporate; this last step was performed several times to dissolve most of the polymer. This elaborate procedure, discussed in detail in a later section, gave reproducible GPC traces and was devised so that the drying process favors trapping of residual water and thus avoids inter- or intramolecular hydrogen bonding of polyNIPAM. The samples were not filtered before analysis for the reason given later.

GPC. Two sets of GPC equipment were used. (1) The first comprised a Waters 210 pump, a differential refractometer (Waters R401), and a control module to set the temperature (typically 27 °C). Two columns were used in series: Ultrastyragel (Waters), linear and 10^3 Å. A 100 μL aliquot of sample at different concentrations was injected at a THF flow rate of 0.6 mL min^{-1}. The calibration curve was obtained with 12 different polystyrene standards, from Polymer Laboratories and Waters, and fitted by a third-order polynomial. (2) The second comprised a Waters liquid chromatograph equipped with a differential refractometer and a set of six Ultrastyragel columns (10^6, 10^5, 10^4, 10^3, 500, and 100 Å) in series. THF (1.0 mL min^{-1}) was used as eluent.

GPC traces were converted to GPC distributions, $w(\log M)$, using the calibration curve in the usual way.[40,41] A comparison of results from both setups will be discussed later. A series of GPC traces are shown in Figure 2 (molecular weights are given in polystyrene equivalents).

A "control" sample, prepared from a NIPAM/benzene polymerization initiated with AIBN (Table 1), was used to investigate the GPC behavior of polyNIPAM. Its actual molecular weight, though not measured here, is believed to be very high and close to that given in the literature for similar conditions; light scattering in THF and water gave $\bar{M}_n \approx 2.5 \times 10^6$ and $\bar{M}_w/\bar{M}_n \approx 8$.[42] The results reported below applied also to samples prepared by polymerization in water using γ-radiolysis initiation or RAFT samples.

In some preliminary experiments, it was found that the presence of water led to well-resolved GPC chromatograms. However, the GPC sample preparation procedure needed refining, as was found by injecting the control polyNIPAM sample prepared for GPC analysis by three different methods: (1) the control was dissolved directly in THF; (2) the control was dissolved in water, dried to completeness, and redissolved in THF (as described above); and (3) the control was dried to completeness (without first dissolving in water) and then dissolved in THF. Chromatograms for the three different sample preparation methods are shown in Figure 3.

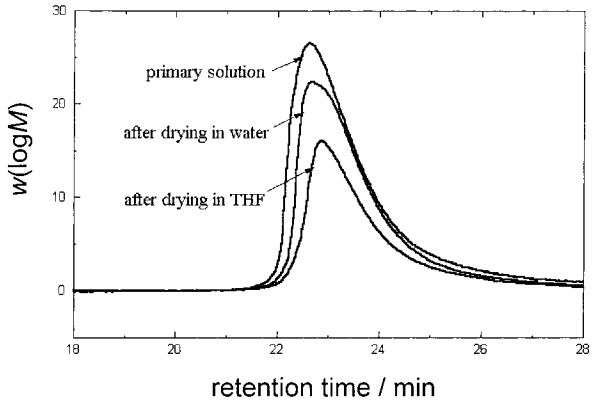

Figure 3. Influence of the sample preparation on polyNIPAM GPC distributions, based on polystyrene standards.

The sample preparation mode clearly has a major effect on the apparent GPC distribution. When the sample is fully dried, polyNIPAM chains can aggregate because of inter- and intramolecular hydrogen bonding, as reported for instance for acrylamide.[42] The fully dried sample dissolved in THF (method 3) shows the smallest signal, an increase in GPC pump pressure, and polymer was seen to collect on the column prefilter. All of these observations are consistent with the presence of residual aggregates which are not fully dissolved in THF; supporting evidence for this comes from a subsequent paper,[43] where osomometry and FTIR showed that the *monomer* undergoes significant dimerization in water solution. When water is added while drying the polymer (method 2), signal intensity increases, suggesting that water separates the polymer chains. However, there is a difference in the peak intensity between the traces from method 2 and those from the primary (or stock) solution (method 1) which may be due to partial redissolution of the long chains in THF, presumably due to the co-nonsolvency effect.[12,13,44] It is postulated that complete drying leads to chain aggregation, which cannot be reversed when the sample is subsequently dissolved in THF (or at least, any deaggregation is very slow). When trace amounts of water become attached to the chains, this prevents "irreversible" hydrogen-bonding interactions between NIPAM units: the residual amounts of water effectively behave as a barrier between chains. Diluting these "protected" chains in THF then eventually removes the residual water. In the following, unless otherwise stated, all the samples have been prepared according to method 2.

The same sample was injected a number of times to check the reproducibility of the GPC technique. Over a week, no variation of the GPC trace and distribution were observed for the same sample. This suggests that, where no aggregates are created, sample preparation produces a solution that is very stable and remarkably soluble in THF, as noted previously by various authors.[14,20,26]

The GPC chromatograms of samples with different molecular weight (from Table 1), Figure 2, show a broadening of the molecular weight distribution with increasing average molecular weight. Furthermore, the shape of the distributions becomes skewed toward the low molecular weight region, together with a cutoff in the high molecular weight region. These asymmetric traces are similar to those given in the literature by Yang et al.[11]

As seen in Figure 3, decreasing the polymer concentration by partial redissolution after drying the sample leads to a different GPC trace. The effect of polyNIPAM concentration on the GPC chromatograms of the control sample (no DTE) in Figure 4 shows that the overall apparent molecular weight distribution shifts toward the high molecular weight region with increasing polymer concentration. This trend has been observed both for the primary solution (method 1) and samples prepared in the presence of water (method 2). It therefore cannot correspond to a solvent effect. Raising the polymer concentration up to the limit presented here (i.e., 0.04 M) led

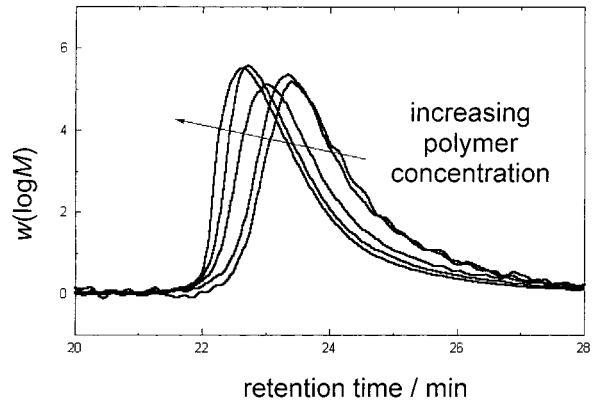

Figure 4. Influence of the polymer concentration of the control sample on the GPC chromatogram (based on polystyrene standards) of the "control" sample (no DTE). The *w*(log *M*) are normalized by dividing the signal by the concentration. The concentration (g of polyNIPAM per dm^3) of each sample are the following (from top to bottom): 4.81, 2.40, 0.928, 0.96, and 0.204.

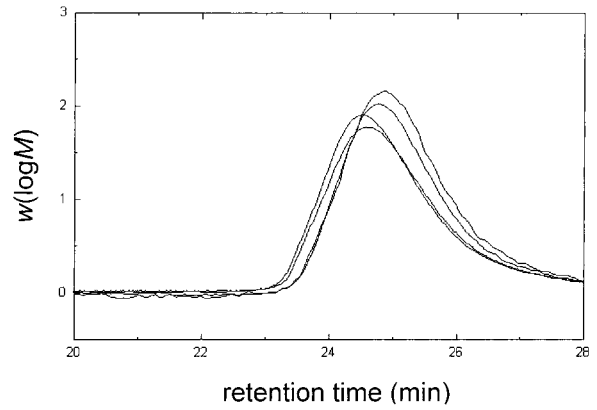

Figure 5. Influence of the polymer concentration of the RAFT sample **1d** on the GPC chromatograms (see Table 1 for details; based on polystyrene standards). Concentrations (g of polyNIPAM per dm^3) as in Figure 4.

to a broader, less resolved GPC trace, which is readily explained by an overloading of the column. The same analysis was performed using a lower molecular weight sample of polyNIPAM prepared by the RAFT process (sample 1d, Table 1), seen in Figure 5. The same variation with concentration was observed as in the absence of DTE, but to a lesser extent. In addition, the peak is much more symmetrical than the control sample.

PolyNIPAM samples were also injected in two different GPC devices, differing in the number of columns (two and six). The six-column system gave better resolved GPC traces and more symmetrical distributions at low molecular weight, thus decreasing the apparent polydispersity index compared to the two-column system. However, the same unsymmetrical shape was observed for high molecular weight and the same tendency to reach a cutoff. The MWDs obtained for a given sample with six rather than two columns were quantitatively very similar except for a slight difference in $\bar{M}_n$. In other words, using a system with more columns merely increases the resolution of the GPC but has no significant effect on the features presented above.

MALDI. Sample **1a** was analyzed in a matrix, comprising 4-hydroxyazabenzene-2′-carboxylic acid (HABA) plus α-cyano-4-hydroxycinnamic acid (HCCA), by a Finnigan Lasermat 2000 MALDI at an acceleration voltage of 25 000 V, pressure of 2.7×10^{-7} Torr, and ~35 scans. The three other samples (namely **1b**, **2a**, and **2b**) were dissolved in THF and mixed with matrices comprising 2,5-dihydroxybenzoic acid (DHB) and NaI salt. They were analyzed on a Perseptive Biosystems Voyager Elite (Framingham, MA), using the following conditions: accelerating voltage 25 000 V, pressure 4.8×10^{-7} Torr, and 255 scans. Only the lowest molecular weight samples (less than 25 000) could be accurately analyzed by MALDI regardless of the matrix or analysis conditions used.

Viscosity Measurements. The samples were dialyzed against water until the residual monomer and impurities contained in the polymer were totally removed (as checked by ^{1}H NMR). They were then injected into a triple-detection SEC device equipped with a Waters 515 HPLC pump, a VE 5200 GPC Autosampler, and a Viscotek differential refractometer/viscometer but no separation columns. This technique is extensively used in industry for rapid polymer characterization. The exact polymer concentration was derived from the refractometry signal, using a differential refractive index value $dn/dc = 0.107$ cm^3 g^{-1}.[20] The intrinsic viscosity was calculated from the specific viscosity (given by the viscometer) and the sample concentration (from the refractometer).

Kinetics. The samples were analyzed by ^{1}H NMR (Bruker 200 MHz) at concentrations of ~10 mg mL^{-1} of polyNIPAM in $CDCl_3$. The conversion was determined by comparisons from the integration of monomer C=C−H (around 6 ppm) with the NH peaks of polymer + monomer at ~ 4 ppm and with the broad alkyl peaks ($CH_3 + CH_2 + CH$) between 0.8 and 2.6 ppm. The average yields given in Table 1 are averages of the two integrations.

Results and Discussion

PolyNIPAM Synthesis Using the RAFT Process. Benzene and 1,4-dioxane were chosen for this work because they are good solvents for polyNIPAM and exhibit low chain-transfer activity to this monomer.[23] It was observed from the polymerization of a control sample (Table 1) that chains with high molecular weights (typically above 10^6) precipitated in benzene; molecular weights in these experiments were therefore kept below this value by controlling the monomer, initiator, and DTE concentrations (Table 1). AIBN was the initiator of choice[31] due to its low decomposition rate (giving a low radical flux and hence minimizing termination) and relatively high efficiency factor in these solvents. The ratios of DTE to initiator concentrations were chosen between 1 and 30, and the initiation rates were kept as low as possible to reduce the rate of radical−radical termination ("ideal" RAFT kinetics would result in all chains having an A-initiated end group, where in the present case A = benzyl or cumyl; see Scheme 1). Conversion and molecular weight data are given in Tables 1 and 2, respectively.

The $\bar{M}_n$ for RAFT can be calculated theoretically[31] by (a) assuming that the efficiency of the dithioester is 100% (i.e., all molecules are attached to a polymer chain end), (b) termination events (chain transfer to monomer and radical−radical termination) are negligible, and (c) the initiation rates are low. One then has

$$\bar{M}_n(\text{theor}) = \frac{[\text{M}]}{[\text{DTE}]} M_0 x \qquad (1)$$

where [M] is the concentration of monomer, x is the fraction conversion, and M_0 is the molecular weight of monomer.

A first test of the applicability of eq 1 is to examine the conversion dependence of $\bar{M}_n$ obtained from GPC (see characterization section above). Figure 6 shows the $\bar{M}_n$ and polydispersity of series 2; $\bar{M}_n$ increases approximately linearly with conversion, suggesting that the RAFT method for NIPAM indeed gives a living polymerization. The theoretical and experimental $\bar{M}_n$ values from MALDI are compared in Table 2 and are in good agreement for molecular weights below ~4 ×

Table 2. PolyNIPAM Molecular Weight Information from the Various Methods Used in This Study (GPC in THF, MALDI, and Online Viscometry)[a]

series	$\bar{M}_n$(theor) (eq 1)	$\bar{M}_n$ exp (MALDI)	$\bar{M}_w/\bar{M}_n$ (MALDI)	$[\eta]$, dL g^{-1}	$\bar{M}_n$(exp) (GPC − rel styrene)	$\bar{M}_w/\bar{M}_n$ (GPC − rel styrene)	$\bar{M}_n$(exp) (GPC − new K,a)	$\bar{M}_w/\bar{M}_n$ (GPC − new K,a)
1a	2.57×10^3	1.90×10^3	1.16		2.25×10^3	1.12	2.03×10^3	1.11
1b	3.97×10^3	3.65×10^3	1.10		3.14×10^3	1.15	2.70×10^3	1.14
1c	3.29×10^4				2.67×10^4	1.21	2.51×10^4	1.19
1d	5.62×10^4				2.77×10^4	1.29	2.61×10^4	1.27
1e	3.31×10^4				2.05×10^4	1.22	1.98×10^4	1.2
2a	7.40×10^3	7.20×10^3	1.17		6.47×10^3	1.14	6.93×10^3	1.13
2b	1.96×10^4	2.05×10^4	1.03	0.131	1.45×10^4	1.20	1.45×10^4	1.18
2c	2.85×10^4			0.169	1.74×10^4	1.37	1.72×10^4	1.33
2d	3.66×10^4			0.213	2.29×10^4	1.43	2.21×10^4	1.4
3a	2.94×10^5			0.927	4.08×10^4	1.51	3.74×10^4	1.46
3b	1.09×10^5			0.466	3.93×10^4	1.53	3.62×10^4	1.49
3c	1.03×10^5			0.509	3.99×10^4	1.59	3.68×10^4	1.54
3d	6.56×10^4			0.315	3.50×10^4	1.44	3.24×10^4	1.43
3e	4.64×10^4			0.291	2.83×10^4	1.50	2.68×10^4	1.45
control					1.45×10^4	1.61	1.45×10^4	1.61

[a] The values of $\bar{M}_n$(exp) and $\bar{M}_w/\bar{M}_n$ from GPC relative to styrene are "raw data", while those with "new K,a" were recalculated from the GPC traces using the Mark−Houwink−Sakaruda parameter values from Figure 9 and Table 3.

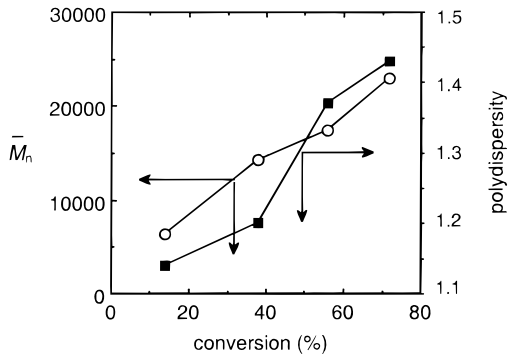

Figure 6. $\bar{M}_n$ and polydispersity ($\bar{M}_w/\bar{M}_n$) from series **2**, as functions of conversion. All molecular weights are relative to styrene. The lines are for visual aid.

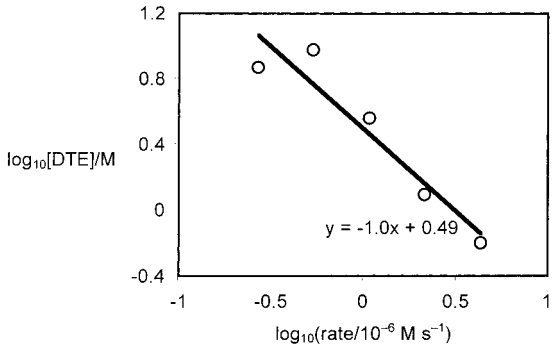

Figure 7. Dependence of rate on dithioester concentration for series **1** of Table 1.

10^4. The polydispersities from GPC (which for the moment are still relative to styrene) were best for the conditions of series 2, remaining below 1.35 up to high conversion (72%). This may be due to the reduction in rates of extraneous processes by any of the cumyl DTE, the solvent (1,4-dioxane), or the high ratio of DTE to AIBN; however, there is also the possibility of a GPC artifact arising from the exclusion limit of the column at the highest molecular weights. More data are needed to make mechanistic inferences.

At first glance, Figure 6 suggests the quantitative applicability of eq 1 and Scheme 1. However, an examination of rate as a function of [DTE] for series 1 (Table 1) suggests that the mechanism is more complex. The rate should remain independent of [DTE], which is not observed, as shown both in Table 1 and in Figure 7. (The rate results given here are subject to large uncertainty, being obtained from minimal data, but the trend is clear.) The decrease in rate with [DTE] might be ascribed to slow reinitiation of polymerization by benzyl radicals (see Scheme 1), leading either to retardation, or to termination with the living radicals, or to slow fragmentation. Since (as exemplified in Figure 7) the rate varies approximately with [DTE]$^{-1}$, termination involving a slowly propagating A·(benzyl or cumyl fragment) is the most likely of these explanations: to some extent, this mean that the DTE RAFT agent also functions as a retarder. A similar effect is also exhibited when cumyl DTE is used: the rate for series 2 is always lower than that of a control sample (a NIPAM/benzene polymerization initiated with AIBN without DTE). The rate decrease cannot be ascribed a priori to a diminution of the gel effect, since the data were obtained at relatively low conversion and in the presence of solvent.

PolyNIPAM Characterization. We now interpret the molecular weight data for the samples analyzed by MALDI, by online viscometry, and by THF-based GPC. The values of $\bar{M}_n$ and polydispersity indices for the different reaction conditions are given in Table 2. The objective here is to obtain reliable Mark−Houwink−Sakaruda parameters, given the anomalies in the literature values.

MALDI. Different samples (samples **1a**, **1b**, **2a**, **2b**; Tables 1 and 2) with low average molecular weights were analyzed by MALDI, using two different devices and experimental conditions (Figure 8). The insets in Figure 8 shows a magnification of the spectrum of sample **1b**. In these matrix conditions, the polymer was adducted by different ions such as H^+, Na^+, and K^+. In addition, two types of chain ends were detected: one with the RAFT agent and the other one with a double bond, originating from dithioester fragmentation. No peaks attributed to AIBN-initiated chains could be detected, which is as expected from "ideal" RAFT kinetics where virtually all chains should have an A (= benzyl or cumyl in the present case) end group; see Scheme 1. This implies that few chains were initiated by AIBN and/or underwent termination, at least for low molecular weights. MALDI analysis was more difficult at higher molecular weights, mainly because the polyNIPAM samples tended to undergo fragmentation.

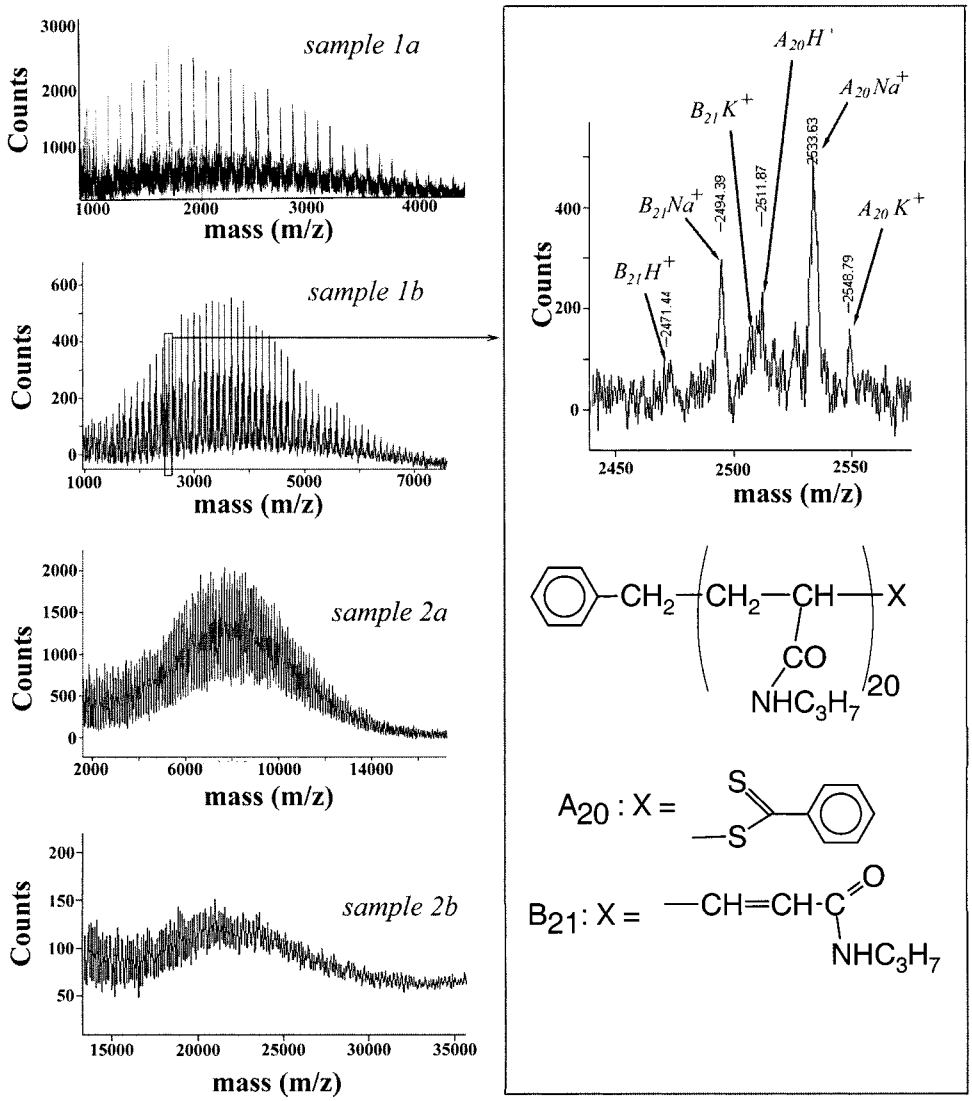

Figure 8. MALDI-TOF analysis of low molecular weight polyNIPAM samples prepared from the RAFT process. Inset: determination of the end-chain structures for sample **1b**.

Values of $\bar{M}_n$ and polydispersity were obtained by appropriate averaging of peak heights. Now, it is essential to be aware that laser ablation in MALDI can have a mass bias,[45] and thus that there is an unknown uncertainty in these values. However, Table 2 shows that acceptable agreement was found between the theoretical $\bar{M}_n$ (eq 1) and MALDI values, and in each case the polydispersity index from MALDI was low (Table 2).

It is pertinent to return to the conversion dependence of the polydispersity shown in Figure 6 in light of the MALDI data. Figure 6 shows that the polydispersity increases with conversion, a result that is inconsistent with ideal RAFT kinetics. For example, the analysis of Muller et al.[46] shows that, if the transfer constant is sufficiently high, then ideal RAFT kinetics imply that polydispersity decreases (while the $\bar{M}_n$ increases) with conversion. The end groups as determined from MALDI suggest that termination occurs (Figure 8 shows double-bond end groups) either by transfer to monomer or through termination by disproportionation, either of which could explain the increase in polydispersity with conversion.

Online Viscometry. For higher molecular weight samples, viscosity measurements were used to gain information on molecular weights (Table 2). The samples were dialyzed against water prior to injection in a triple-detector SEC device with no columns set up (see Experimental Section). Mark−Houwink−Sakaruda values given in the literature for polyNIPAM chains in THF (Table 3) did not give reasonable values for low molecular weight.These parameters were thus recalculated as follows. The acceptable agreement between the values of $\bar{M}_n$ expected from eq 1 and those determined from MALDI (Table 2) and the relatively small polydispersity from GPC (relative to styrene, also given in Table 2) suggest the applicability of "ideal" RAFT

Table 3. Mark−Houwink−Sakaruda Parameters for PolyNIPAM for Different Solvents and Temperatures[a]

solvent	temp, °C	K, dL g^{-1}	*a*	MWD method	ref
water	20	1.12×10^{-3}	0.51	LS[a]	19
water	20	1.45×10^{-3}	0.50	OS[b]	26
water	20	0.46×10^{-5}	0.93	LS	18
water	25	0.23×10^{-5}	0.97	LS	18
methanol	25	3.0×10^{-4}	0.64	LS	18
THF	27	9.6×10^{-5}	0.65	OS	26
THF	27	$10^{-(4.24\pm0.42)a}$	0.78 ± 0.09	RAFT process	this work

[a] Mean 5.8×10^{-5}, range $(2.2-15) \times 10^{-5}$.

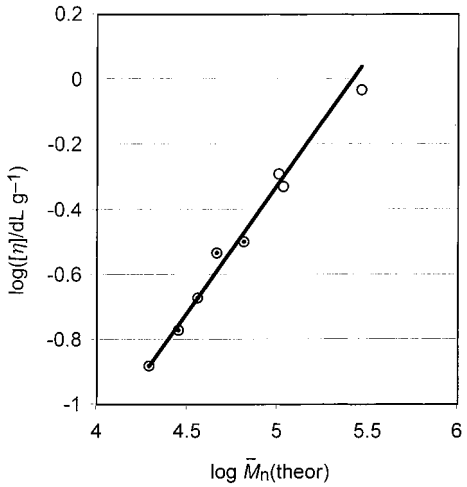

Figure 9. Points: intrinsic viscosity [η] as a function of polyNIPAM $\bar{M}_n$(theor) predicted from RAFT model, eq 1. Line: least-squares fit for data points with $\bar{M}_n < 10^5$ (filled points).

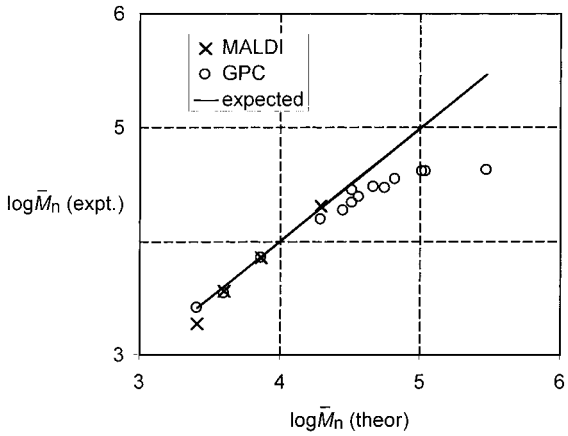

Figure 10. Points: comparison of values of $\bar{M}_n$ predicted from the RAFT relation, eq 1, with those obtained experimentally from MALDI and from GPC using the values of K and a deduced from Figure 9. Line: values expected if all three methods gave same result.

conditions, at least for lower molecular weights. The MALDI data thus suggest that the values of $\bar{M}_n$(theor) should be reliable, at least for lower molecular weights. Figure 9 gives a log/log plot of intrinsic viscosity as a function of $\bar{M}_n$(theor), i.e., the value of $\bar{M}_n$ expected from eq 1. The Mark−Houwink−Sakaruda parameters for polyNIPAM were obtained from this plot with data restricted to $M < 10^5$. The values (with 95% confidence intervals) over this range of M ($2 \times 10^4 \leq M \leq 10^5$) are $K = 10^{-(4.24\pm0.42)}$ dL g^{-1} (the mean value in this confidence interval being 5.8×10^{-5} and the range being $(2.2-15) \times 10^{-5}$ dL g^{-1}) and $a = 0.78 \pm 0.09$.

Corrected GPC Distributions. The GPC data for polyNIPAM, which give molecular weight distribution relative to styrene, can now be converted to true molecular weights using the usual universal calibration method, based on the relationship

$$\text{hydrodynamic volume} = [\eta]M = KM^{a+1} \qquad (2)$$

with $K = 11.4 \times 10^{-5}$ dL g^{-1} and $a = 0.716$ for styrene.[47] Values of $\bar{M}_n$ and polydispersity obtained from this recalculation are given in Table 2.

Figure 10 compares the GPC $\bar{M}_n$ values so obtained with those from MALDI and from eq 1. While there is good agreement between the $\bar{M}_n$ predicted from eq 1 and those observed (directly or indirectly) for lower molecular weights (Table 1, series 1 and 2), discrepancies arise for higher molecular weights (series 3). As expected, polydispersity indices increase both with conversion (Figure 6) and with $\bar{M}_n$ (Table 2). RAFT is "well behaved" only if the molecular weight of polymer produced is substantially lower than that in a control experiment (i.e., in the absence of transfer agent). Thus, compared to the control, the deviations from ideal living behavior for the higher molecular weight samples in series 1, and all of series 3, are to be expected and may be readily ascribed to termination, etc.

Discussion of GPC Characterization of NIPAMs. The various results dealing with GPC characterization of polyNIPAM are now summarized. It would appear that incomplete drying of polymer (trace amounts of residual water) and then dissolving in THF prevents interactions between chains and therefore permits some control of the aggregation process. This technique leads to reproducible GPC results. In the high molecular weight range, GPC traces exhibit an unsymmetrical shape and a cutoff limit, where no separation of the polymer occurs, which is not expected in SEC. In addition, the apparent GPC distribution shifts toward high molecular weights with increasing sample concentration. On the other hand, almost symmetrical distributions and insignificant concentration effects occur in the low molecular weight domain, and the GPC polydispersity is in acceptable agreement with that obtained from MALDI.

The internal inconsistencies in GPC results with increasing concentrations etc. (Figures 3−5) cannot be trivially due to the GPC technique. Polystyrene standards with different molecular weights to cover the range of polyNIPAM used here were injected at different concentrations, and no variations of the peak retention were observed. No column overloading was observed with the concentrations of polystyrene standards employed, although this effect started to become apparent if higher polymer concentrations were used. In addition, the calibration curve was unchanged with time. Another explanation might be that the polyNIPAM chains precipitated on the columns. However, injections at different concentrations were reproducible, in the sense that normalization gave the same area for each peak, although the shape of the peak differed slightly with concentration. This suggests that there is no loss of polymer, and some other process must occur during the separation on the column.

The results obtained here suggest that discrepancies found in the literature between the THF-based GPC and viscometry/light scattering methods might arise from effects of the sample concentration and pressure on the polymer chains. Both light scattering and viscometry give a molecular weight value by extrapolating to infinite dilution, whereas GPC is performed at comparatively high concentrations and pressure. This explanation also supports the necessity of not filtering the samples before GPC analyses.[7]

It is suggested that GPC characterization of polymers such as NIPAM requires (i) centrifugation of the samples prior to analysis rather than filtration (to ensure that no polymer loss occurs) and (ii) injection in a low-shear-gradient GPC device. This condition requires either working at low elution rate or decreasing the shear

gradient by setting up the apparatus with tubing twice the diameter generally used.

These precautions should ensure that the GPC gives reliable results either by online viscometry detection (or, better, triple-detector SEC) or by preparing standards from controlled radical polymerization.

Conclusions

This article reports the first use of the RAFT process to polymerize NIPAM. A range of relatively monodisperse polymer samples were obtained with molecular weights ranging from 2×10^3 to 4×10^5. The living nature of the polymerization process was assessed by looking at different parameters, such as the influence of the type of dithioester used, the reaction solvent, the initiator concentration, and the evolution of the molecular weight with conversion.

The living process is efficient, regardless of the solvent or dithioester used, at least for low molecular weights, where there is good agreement between the molecular weight calculated assuming ideal living polymerization and that obtained experimentally. The transfer constant of the dithioesters is high enough to limit the formation of new chains, even at high AIBN concentration. In addition, transfer and termination of the chains are sufficiently slow to lead to a relatively low polydispersity. A decrease of the polymerization rate with amount of chain-transfer agent was observed. This can be ascribed to a slow reinitiation of the RAFT-derived radical (benzyl or cumyl in this case) with NIPAM monomer leading to termination.

Particular care is required when preparing polyNIPAM samples for organic-phase GPC analysis with THF as solvent: polymer must be dried in the presence of water and then dissolved in THF to prevent irreversible chain aggregation. MALDI-TOF and GPC give similar molecular weight distributions (at least for the low molecular weight samples analyzed), whereas discrepancies arose for higher molecular weight (comparing GPC and viscometry data). The molecular weight distributions are broader for higher average molecular weights, and the apparent GPC average molecular weights seem to reach a plateau value, albeit the calculated one. Despite this inherent GPC problem, the characterization of polyNIPAM by the present combination of intrinsic viscosity and MALDI data on RAFT samples yields Mark−Houwink parameters for molecular weights below 10^5. The GPC approach used checks for internal consistency for molecular weights inferred from three independent methods: viscosity (linear Mark−Houwink plots), MALDI, and theoretical RAFT molecular weights.

Acknowledgment. F.G. gratefully acknowledges the support of an Australian Research Council International Exchange Fellowship and of an Innovalyon award. The Key Centre for Polymer Colloids is established and supported under the Australian Research Council's Research Centres Program.

References and Notes

(1) Han, C. K.; Bae, Y. H. *Polymer* **1998**, *39*, 2809.
(2) Ding, Z.; Chen, G.; Hoffman, A. S. *Bioconjugate Chem.* **1996**, *7*, 121.
(3) Yasui, M.; Shiroya, T.; Fujimoto, K.; Kawaguchi, H. *Colloids Surf. B: Biointerfaces* **1997**, *8*, 311.
(4) Terada, T.; Inaba, T.; Kitano, H.; Maeda, Y.; Tsukida, N. *Macromol. Chem. Phys.* **1994**, *195*, 3261.
(5) Pelton, R. *Adv. Colloid Interface Sci.* **2000**, *85*, 1.
(6) Tiktopulo, E. I.; Uversky, V. N.; Lushchik, V. B.; Klenin, S. I.; Bychkova, V. E.; Ptitsyn, O. B. *Macromolecules* **1995**, *28*, 7519.
(7) Wu, X. Y.; Pelton, R. H.; Tam, K. C.; Woods, D. R.; Hamielec, A. E. *J. Polym. Sci., Part A: Polym. Chem.* **1993**, *31*, 957.
(8) Schild, H. G. *Prog. Polym. Sci.* **1992**, *17*, 163.
(9) Cole, C.-A.; Schreiner, S. M.; Priest, J. H.; Monji, N.; Hoffman, A. S. *ACS Symp. Ser.* **1987**, *350*, 245.
(10) Chen, G.; Hoffman, A. S. *Macromol. Chem. Phys.* **1995**, *196*, 1251.
(11) Yang, H. J.; Cole, C.-A.; Hoffman, A. S. *J. Polym. Sci., Part A: Polym. Chem.* **1990**, *28*, 219.
(12) Schild, H. G.; Muthukumar, M.; Tirell, D. A. *Macromolecules* **1991**, *24*, 948.
(13) Winnik, F. M.; Ottaviani, M. F.; Bossmann, S. H.; Garcia-Garibay, M.; Turro, N. J. *Macromolecules* **1992**, *25*, 6007.
(14) Winnik, F. M.; Davidson, A. R.; Hamer, G. K.; Kitano, H. *Macromolecules* **1992**, *25*, 1876.
(15) Schild, H. G. *ACS Symp. Ser.* **1991**, *467*, 249.
(16) Park, T. G.; Hoffman, A. S. *Macromolecules* **1993**, *26*, 5045.
(17) Hofkens, J.; Hotta, J.; Sasaki, K.; Masuhara, H.; Iwai, K. *Langmuir* **1997**, *13*, 414.
(18) Chiantore, O.; Guaita, M.; Trossarelli, L. *Makromol. Chem.* **1979**, *180*, 2019.
(19) Kubota, K.; Fujishige, S.; Ando, I. *Polym. J.* **1990**, *22*, 15.
(20) Zhou, S.; Fan, S.; Au-Yeung, S. C. F.; Wu, C. *Polymer* **1995**, *36*, 1341.
(21) Norisuye, T.; Shibayama, M.; Nomura, S. *Polymer* **1998**, *39*, 2769.
(22) Winnik, F. M. *Macromolecules* **1990**, *23*, 233.
(23) Min, Y.; Jun, L.; Hongfei, H. *Radiat. Phys. Chem.* **1995**, *46*, 855.
(24) Tam, K. C.; Wu, X. Y.; Pelton, R. H. *Polymer* **1992**, *33*, 436.
(25) Tam, K. C.; Wu, X. Y.; Pelton, R. H. *J. Polym. Sci., Part A: Polym. Chem.* **1993**, *31*, 963.
(26) Fujishige, S. *Polym. J.* **1987**, *19*, 297.
(27) Zammit, M. D.; Davis, T. P. *Polymer* **1997**, *38*, 4455.
(28) Jackson, C. *Polymer* **1999**, *40*, 3735.
(29) Webster, O. W.; Hertler, W. R.; Sogah, D. Y.; Farnham, W. B.; RajanBabu, T. V. *J. Am. Chem. Soc.* **1983**, *105*, 5706.
(30) Teodorescu, M.; Matyjaszewski, K. *Macromolecules* **1999**, *32*, 4826.
(31) Chiefari, J.; Chong, Y. K.; Ercole, F.; Krstina, J.; Le, T. P. T.; Mayadunne, R. T. A.; Meijs, G. F.; Moad, G.; Moad, C. L.; Rizzardo, E.; Thang, S. H. *Macromolecules* **1998**, *31*, 5559.
(32) Rizzardo, E.; Chiefari, J.; Chong, Y. K.; Ercole, F.; Krstina, J.; Jeffery, J.; Le, T. P. T.; Mayadunne, R. T. A.; Meijs, G. F.; Moad, G.; Moad, C. L.; Thang, S. H. *Macromol. Symp.* **1999**, *143*, 291.
(33) Mayadunne, R. T. A.; Rizzardo, E.; Chiefari, J.; Chong, Y. K.; Moad, G.; Thang, S. H. *Macromolecules* **1999**, *32*, 6977.
(34) Chong, Y. K.; Le, T. P. T.; Moad, G.; Rizzardo, E.; Thang, S. H. *Macromolecules* **1999**, *32*, 2071.
(35) Hawthorne, D. G.; Moad, G.; Rizzardo, E.; Thang, S. H. *Macromolecules* **1999**, *32*, 5457.
(36) Solomon, D. H.; Rizzardo, E.; Cacioli, P. US Patent 4,581,-429 (*Chem. Abstr.* **1985**, *102*, 221335q).
(37) Wang, J.-S.; Matyjaszewki, K. *Macromolecules* **1995**, *28*, 7901.
(38) Thang, S. H.; Chong, Y. K.; Mayadunne, R. T. A.; Moad, G.; Rizzardo, E. *Tetrahedron Lett.* **1999**, *40*, 2435.
(39) Le, T. P.; Moad, G.; Rizzardo, E.; Thang, S. H. Polymerization with living characteristics with controlled dispersity, polymers prepared thereby, and chain-transfer agents used in the same. WO Patent 9801478 9801478, 1998.
(40) Shortt, D. W. *J. Liq. Chromatogr.* **1993**, *16*, 3371.
(41) Clay, P. A.; Gilbert, R. G. *Macromolecules* **1995**, *28*, 552.
(42) Ying, Q.; Wu, G.; Chu, B.; Farinato, B.; Jackson, L. *Macromolecules* **1996**, *29*, 4646.
(43) Ganachaud, F.; Balic, R.; Monteiro, M. J.; Gilbert, R. G. *Macromolecules*, submitted.
(44) Winnik, F. M.; Ottaviani, M. F.; Bossmann, S. H.; Pan, W.; Garcia-Garibay, M.; Turro, N. J. *Macromolecules* **1992**, *26*, 4577.
(45) Axelsson, J.; Scrivener, E.; Haddleton, D. M.; Derrick, P. J. *Macromolecules* **1996**, *29*, 8875.
(46) Muller, A. H. E.; Zhuang, R. G.; Yan, D. Y.; Litvinenko, G. *Macromolecules* **1995**, *28*, 4326.
(47) Brandrup, J.; Immergut, E. H.; Grulke, E. A. In *Polymer Handbook*, 4th ed.; Brandrup, J., Immergut, E. H., Grulke, E. A., Eds.; John Wiley & Sons: New York, 1999.

MA0003102